

Data

Major and trace element abundances in <180 and 180-2000 μm fractions of stream sediments from the Hii River, Shimane Prefecture, Japan

Edwin Ortiz* and Barry Roser*

Abstract

Stream sediments collected from 47 localities in the Hii River of Shimane Prefecture were hand sieved to separate the <180 μm and 180-2000 μm fractions. Major and trace compositions of both fractions in each sample were determined by X-ray fluorescence analysis. Elemental abundances contrast significantly between the two size fractions. Average abundances of SiO₂, K₂O, Ba, and Rb are greater in the 180-2000 μm fractions, whereas the remaining elements are generally more abundant in the <180 μm fractions. Loss on ignition values are also greater in the <180 μm fractions. Average compositions of both fractions show similar normalized distributions to average upper continental crust. The greatest departure from upper continental crust composition is observed in the <180 μm fraction, with enrichment for several ferromagnesian elements (V, TiO₂, Fe₂O₃, Sc) and for Zr, Y, and Th. In both fractions, Nb, CaO, Na₂O, Sr, Rb, MgO and Ni are slightly depleted relative to UCC.

Key words: Stream sediments, Hii River, geochemistry, major and trace elements

Introduction

Although elemental abundances in the composition of stream sediments reflect the geochemical characteristics of lithotypes present in their catchment, they are also influenced by a variety of processes that operate between the source and the sediments produced. Such processes include weathering, size sorting, heavy mineral placering effects, and the effects of addition of detritus from geochemically disparate source rocks. The factors involved in these processes have been the subject of numerous studies (e.g. Basu et al. 1990; Johnson, 1993; Ohta et al. 2004; Avila et al. 2005) because they provide information crucial for the interpretation of phenomena of geological and environmental interest.

This article reports X-ray fluorescence (XRF) analyses of <180 μm and 180-2000 μm fractions of 47 stream sediment samples collected from the Hii River. The Hii drainage system is located in eastern Shimane Prefecture, and drains an area of about 930 km² over a main channel length of approximately 82 km, stretching from the headwaters in Mount Sentsu to the western end of Lake Shinji (Fig. 1). The Hii River supplies a major proportion of the sediments entering the Lake Shinji-Lake Nakaumi coastal lagoon system. The historical, cultural, social, environmental and economic importance of this area has been reviewed by Tokuoka et al. (1998).

The purpose of this report is to present the data obtained by XRF analysis, along with a brief description of the general variations of elemental abundances in two size fractions of sediments from the Hii River. More extensive

and specific discussion will be published at a later date. The dataset presented here is part of a regional geochemical database for the northern San'in region. This project began with the study of the Kando and the Hino Rivers (Ortiz and Roser 2003; Ortiz and Roser 2004a, b) and greatly increases (by over ten times) the density of geochemical data available for stream sediments in the area.

Lithology of the Hii River Basin

In the regional context the distribution of lithological units in the Hii River drainage basin is relatively simple. Cretaceous to Paleogene felsic to intermediate granitoids and volcanic rocks extend throughout most of the catchment (Fig. 1). Granitoids occupy the majority of the central basin, whereas less extensive volcanic rocks are concentrated towards the southern edge of the watershed. Lithotypes among the plutonic rocks include granodiorites, granites, granite porphyries, granophyres and quartz diorites to gabbros, whereas the volcanic rocks are mainly dacite to rhyolite lavas and pyroclastics (Editorial Board of Geological Map of Shimane Prefecture "EBGMSP" 1997).

A second group of lithological units including Miocene volcanic and sedimentary rocks, principally of the Hata, Kawai, Kuri, Omori, and Fujina Formations, crops out along the western boundary and in the northeastern extremity of the drainage basin (Fig. 1). The main lithotypes are rhyolite to dacitic lavas, andesites, and pyroclastic rocks, along with locally derived sandstones, conglomerates and shales (EBGMSP 1997).

The characteristics and interrelationships among most of the units cropping out in this drainage basin have been described in a number of studies (e.g. Iizumi et al., 1984,

*Dept. of Geoscience, Shimane University, Matsue 690-8504, Japan

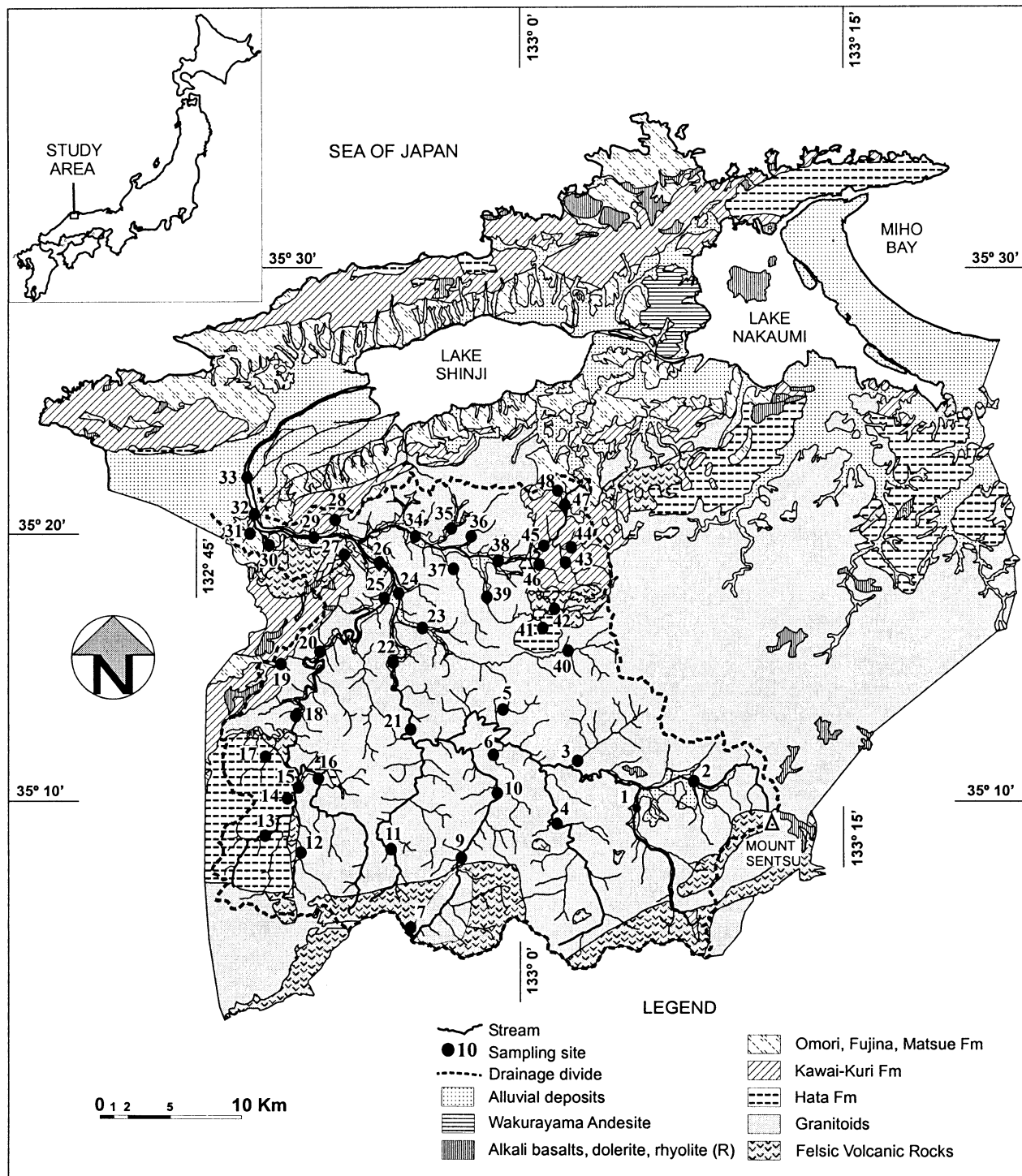


Fig. 1. Map showing the generalized distribution of lithotypes in the catchment of the Hii River and location of sample sites. Geology based on the 1:200,000 geological map of Shimane Prefecture (Editorial Board of Geological map of Shimane Prefecture, 1997).

Kagami et al., 1992; Yamauchi and Yoshitani, 1992; Kano et al., 1994; Roser et al., 2001).

Sampling and Sample Preparation

Field Sampling

Sampling was carried out on five days during autumn

2004. Weather conditions were clear and dry, and stream flows normal. Sub-samples were collected with a plastic water scoop from active channels over a length of 20–50 m, and then stored in plastic zip-top bags as single representative samples for each site.

Selection of sampling sites was made with the aim of achieving a uniform distribution that would cover all

lithological units present in the drainage system. Localities were selected from 1:50,000 topographic base maps on which geology from the 1:200,000 geological map of Shimane Prefecture (EBGMSP 1997) had been overlain. At a few localities samples could not be collected due to difficulty of access or paucity of sand-grade sediment, and sites were displaced slightly from those originally intended. Location of the sampling sites is given in Figure 1. Overall sampling density was one sample per 19.7 km².

Sample Preparation

Bulk samples were dried at 80–90°C the day after collection, and subsequently hand-sieved to remove pebbles and clasts coarser than 2 mm. Average weight of the <2 mm fractions was 993 g. These <2 mm fractions were split (mostly into eighths or quarters), and an appropriately sized split was then passed through an 83 mesh stainless steel sieve to separate the <180 and 180–2000 µm fractions. On average, the <180 µm fraction comprised 12 wt% of the <2 mm bulk material. Only in four samples did the <180 µm fraction exceed 20 wt%. The <180 µm fraction formed a particularly large proportion (70 wt%) of the sample collected at site 31.

Both fractions were then crushed separately in tungsten carbide mills, applying the procedures described in Ortiz and Roser (2004b). Sub-samples (10–12 g) of the crushed fractions were then placed in glass vials and dried for at least 24 hours at 110°C prior to determination of loss on ignition (LOI).

Analytical Methods

LOI was estimated for each sample from the net weight loss after ignition in a muffle furnace at 1000°C for at least two hours. Ignited materials were returned to glass vials and held at 110°C for at least 24 hours before the preparation of fusion beads for XRF analysis (anhydrous basis).

Major elements and 14 trace elements (Ba, Ce, Cr, Ga, Nb, Ni, Pb, Rb, Sc, Sr, Th, V, Y, Zr) were determined from glass beads, prepared with a flux (80% lithium tetraborate and 20% lithium metaborate) to sample ratio of 2:1. Analyses were made using a Rigaku RIX-2000 XRF spectrometer at Shimane University, and following the methods, instrument conditions, and calibrations described by Kimura and Yamada (1996). More detailed descriptions of the methods used are given by Roser et al. (2000, 2001) and Ortiz and Roser (2003, 2004a, b).

Results

Major and trace element analyses of the <180 µm and 180–2000 µm fractions are listed in Tables 1 and 2, respectively. Data are listed on a hydrous basis, with total iron expressed as Fe₂O₃. LOI values in both fractions were low, in all cases less than 10 wt%. In the <180 µm fractions only 14 samples

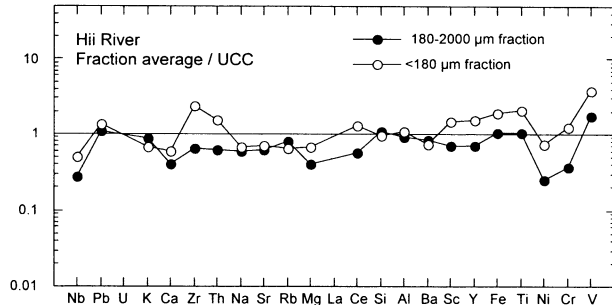


Fig. 2. Multi-element plot showing the average composition (anhydrous normalized) of <180 and 180–2000 µm fractions from the Hii River (data from Table 3) normalized against the Upper Continental Crust (UCC) average of Taylor & McLennan (1985). Elements are arranged from left to right in order of increasing normalized abundance in average Mesozoic-Cenozoic greywacke (Condie 1993) relative to UCC, following the methodology of Dinelli et al. (1999). The major elements are normalized as oxides.

had LOI values > 5 wt%, whereas in the 180–2000 µm fractions values were considerably lower, with most samples < 2 wt%, and only two exceeding 5 wt%.

Summary statistics for the fractions from analyses normalized to 100% LOI-free are given in Table 3. Contrast in average elemental abundances between the fractions is significant. Abundances of most of the elements analyzed are greater in the <180 µm average, except for SiO₂, K₂O, Ba, and Rb, which have higher values in the 180–2000 µm fraction. Although there are several anomalies, the average composition over the entire suite is similar to that of average upper continental crust (UCC), as shown in Figure 2. The 180–2000 µm fraction average is slightly depleted in most elements relative to UCC, and only shows slight enrichment in Pb, Ce and V. The pattern is relatively flat overall, and greatest depletion is seen in Nb, Ni, Cr, CaO and MgO. In contrast, the <180 µm fraction average is a little less regular, exhibiting both enrichment and depletion relative to UCC. The largest departure of the <180 µm fraction average from UCC composition is seen in the enrichment of V and the segments Zr-Th and Sc-Ti. Nb and several mobile elements (CaO, Na₂O, Sr, Rb, MgO) are depleted relative to UCC, as they are in the 180–2000 µm fraction average. In general, however, the patterns of the fraction averages are very similar to those shown by equivalent size fractions from the neighbouring Kando and Hino rivers (Ortiz and Roser 2003, 2004a, b).

Conclusions

Average chemical compositions of <180 and 180–2000 µm fractions of stream sediments from the Hii River show significant contrasts in abundances. LOI and average abundances of most elements are generally greater in the <180 µm fractions, but the 180–2000 µm fractions have higher average contents of SiO₂, K₂O, Ba and Rb. Average compositions of both fractions are similar to that of the

Table 1. Major and trace element analyses of the <180 μ m fractions, Hii River (hydrous basis). Major elements wt%, trace elements ppm.

SaNr	SiO ₂	TiO ₂	Al ₂ O ₃	Fe ₂ O ₃ t	MnO	MgO	CaO	Na ₂ O	K ₂ O	P ₂ O ₅	LOI	SUM	Ba	Ce	Cr	Ga	Nb	Ni	Pb	Rb	Sc	Sr	Th	V	Y	Zr	% <180 μ m
HII-1	66.37	0.50	15.79	3.68	0.13	0.95	2.11	3.72	2.73	0.08	2.90	98.96	476	73	14	18	11	7	23	92	9.3	211	13.1	49	34	269	14.5
HII-2	57.35	1.06	14.81	13.11	0.22	1.58	3.14	3.86	2.29	0.09	1.49	99.02	386	163	42	17	25	9	12	68	22.6	203	52.3	266	79	983	20.8
HII-3	60.48	0.76	16.75	8.65	0.17	0.96	2.26	4.39	2.72	0.09	2.08	99.33	333	151	23	19	21	7	13	91	9.3	239	50.0	156	57	749	24.8
HII-4	65.38	0.59	16.34	4.65	0.13	0.98	2.22	4.00	2.66	0.06	2.10	99.31	463	79	15	18	13	8	18	94	7.8	234	13.7	73	30	271	9.6
HII-6	60.79	0.57	18.61	4.70	0.17	1.29	2.75	4.41	2.63	0.12	3.41	99.44	399	94	20	20	12	10	18	88	11.7	282	21.8	80	36	346	10.2
HII-7	57.12	0.81	16.45	6.37	0.16	1.89	3.35	2.12	1.79	0.14	8.86	99.07	347	52	39	20	9	28	19	57	12.1	436	6.3	117	19	256	12.9
HII-9	61.12	1.12	13.87	11.56	0.24	1.01	2.07	3.29	2.58	0.09	1.88	98.84	405	103	56	17	17	26	39	72	10.7	213	20.7	224	34	484	4.6
HII-10	52.69	1.48	12.44	21.33	0.29	1.15	2.43	3.15	2.24	0.11	0.83	98.14	376	209	68	19	26	16	25	58	13.1	199	59.5	450	59	1216	2.4
HII-11	57.86	1.32	13.41	14.38	0.32	1.41	2.64	2.36	2.59	0.07	21.9	98.56	419	114	55	20	18	19	64	76	9.5	308	17.4	286	25	848	5.5
HII-12	57.73	1.95	12.98	14.88	0.28	1.67	2.82	2.36	1.89	0.05	2.03	98.65	349	64	62	17	15	13	24	51	16.8	301	11.1	554	22	484	15.7
HII-13	60.21	0.91	17.04	7.43	0.17	1.45	2.92	2.07	1.53	0.10	5.37	99.21	336	37	19	18	7	10	24	47	18.6	376	6.0	171	21	175	12.3
HII-14	60.02	0.81	16.61	7.72	0.18	1.59	2.81	1.96	1.20	0.09	6.22	99.21	309	35	27	18	6	11	19	34	17.5	369	5.2	173	19	175	11.4
HII-15	58.85	1.53	14.68	12.12	0.20	1.56	2.94	2.31	1.80	0.07	2.76	98.83	358	46	38	17	9	12	25	50	17.4	354	8.8	388	18	294	11.4
HII-16	64.32	1.24	13.13	9.97	0.20	1.15	2.14	2.07	2.47	0.06	2.01	98.75	382	63	20	15	11	9	30	68	12.5	247	10.8	303	21	304	11.6
HII-17	59.59	0.85	16.08	9.25	0.16	1.50	3.57	1.99	1.31	0.10	4.62	99.04	302	40	43	19	6	18	21	33	17.8	392	5.0	215	20	199	6.7
HII-18	62.38	1.12	14.57	9.38	0.17	1.37	2.59	2.37	2.14	0.08	2.86	99.03	367	54	31	16	9	8	26	62	14.1	303	8.3	259	19	318	10.2
HII-19	64.25	1.77	12.90	10.62	0.17	1.02	1.50	1.79	1.82	0.07	2.85	98.75	326	72	36	16	11	9	24	54	15.1	182	9.9	300	27	393	9.2
HII-20	62.41	1.04	14.83	9.01	0.16	1.33	2.62	2.88	2.27	0.09	2.49	99.13	389	64	32	16	10	8	26	63	13.9	298	10.3	241	25	320	17.9
HII-21	60.30	0.93	15.51	9.09	0.18	1.85	3.42	3.66	2.42	0.11	1.77	99.24	362	90	27	17	14	9	16	77	17.0	285	23.7	198	38	435	12.3
HII-22	62.76	0.90	16.15	6.77	0.17	1.94	3.40	3.57	2.49	0.12	0.90	99.18	378	74	32	18	12	12	23	80	19.2	282	14.6	149	35	271	5.4
HII-23	60.36	1.02	13.61	12.65	0.18	1.45	2.53	3.42	2.93	0.14	8.86	99.16	306	173	53	16	25	11	12	95	15.0	203	50.3	259	79	1177	19.2
HII-24	56.82	1.20	14.65	12.36	0.22	1.94	2.92	3.16	2.46	0.12	2.38	99.13	377	102	60	17	17	19	15	77	17.5	233	22.5	313	42	614	6.5
HII-25	56.39	1.54	13.08	16.64	0.21	1.52	2.57	2.83	2.14	0.10	1.52	98.54	347	125	64	15	14	11	21	54	15.1	246	21.0	481	32	948	14.2
HII-26	59.96	1.08	14.82	10.53	0.19	1.63	2.67	3.00	2.35	0.11	2.67	99.02	387	85	45	17	13	13	22	66	15.4	257	14.1	263	30	456	6.6
HII-27	63.13	1.07	15.40	7.03	0.29	1.23	1.77	1.88	2.34	0.10	4.76	99.01	417	54	39	18	7	17	23	82	17.3	183	9.4	156	24	234	7.0
HII-28	57.66	1.44	16.03	8.28	0.21	1.58	2.33	1.65	1.29	0.05	8.37	99.00	372	57	25	20	11	10	35	21.7	230	4.5	157	34	274	6.6	
HII-29	58.84	0.72	18.12	6.02	0.27	1.87	2.50	2.66	2.46	0.16	5.76	99.37	432	72	30	20	10	20	25	84	15.8	233	13.3	90	31	285	2.4
HII-30	61.17	0.91	15.30	7.08	0.22	1.56	2.28	1.59	2.05	0.15	6.64	98.94	438	58	44	17	10	18	74	13.3	195	6.8	133	26	306	5.5	
HII-31	57.86	0.84	19.23	7.78	0.13	1.61	1.56	0.36	0.80	0.07	9.27	99.52	362	42	20	20	7	8	19	30	22	156	5.1	164	24	196	69.9
HII-32	56.96	0.86	16.98	8.33	0.26	1.67	2.19	2.38	2.35	0.19	6.96	99.12	442	84	27	20	12	13	30	82	16.1	205	18.4	157	38	346	11.3
HII-33	62.72	0.64	16.46	6.54	0.20	1.26	2.34	3.44	2.96	0.09	2.71	99.35	467	72	41	17	10	19	19	96	10.9	236	15.6	126	27	345	0.6
HII-34	54.41	0.90	14.08	16.56	0.21	1.99	2.60	2.72	2.23	0.18	2.95	98.83	387	105	132	16	10	21	18	59	15.5	216	17.2	379	35	888	11.1
HII-35	62.18	0.66	15.71	6.87	0.15	1.99	2.96	3.11	2.54	0.11	2.75	99.04	384	72	44	16	8	18	20	64	16.2	257	12.7	128	26	476	8.4
HII-36	57.94	0.89	15.39	11.19	0.18	2.22	3.06	3.27	2.43	0.17	2.49	99.23	407	113	104	15	11	29	67	18.3	265	21.4	237	34	762	6.0	
HII-37	58.69	0.69	16.41	7.57	0.19	2.15	3.38	3.47	2.48	0.22	3.86	99.11	408	85	52	18	9	26	66	14.8	290	14.0	130	34	476	2.9	
HII-38	63.03	1.11	13.69	9.51	0.17	1.49	2.29	1.65	1.70	0.04	9.79	99.21	446	52	8	14	9	4	28	88	5.0	173	11.1	101	20	173	95.4
HII-39	63.10	0.92	13.73	0.18	0.69	1.62	2.72	2.95	0.07	0.28	98.52	482	146	31	16	19	4	18	80	6.8	180	29.3	272	36	325	9.76	
HII-41	63.37	1.02	11.44	14.43	0.25	0.86	1.77	1.92	2.62	0.04	0.78	98.50	434	61	48	20	12	12	48	81	4.4	264	11.5	308	14	230	94.5
HII-42	67.26	1.01	11.80	9.85	0.16	0.98	2.04	2.17	2.38	0.03	0.92	98.60	414	33	39	15	7	6	26	64	6.2	299	4.9	347	11	120	84.3
HII-43	64.95	0.59	16.84	9.46	0.13	1.14	2.48	2.36	2.05	0.06	3.65	99.21	438	28	7	17	5	4	25	59	14.2	391	5.8	102	15	123	87.7
HII-44	65.62	0.54	15.67	5.57	0.15	1.30	2.12	2.09	1.81	0.07	3.67	98.61	395	31	10	17	5	4	19	46	13.6	303	3.9	111	16	132	88.6
HII-45	66.34	0.89	13.94	7.35	0.13	1.02	2.52	2.54	2.22	0.05	1.70	98.71	422	32	23	15	6	7	21	63	9.9	390	5.5	223	12	103	88.6
HII-46	71.57	0.77	15.16	9.68	0.15	1.34	2.65	1.75	1.70	0.08	3.14	98.83	350	33	24	18	6	5	18	44	14.7	293	5.5	214	17	140	93.3
HII-47	71.51	0.50	13.38	4.10	0.1																						

Table 3. Summary statistics for all <180 and 180-2000 μm fractions (anhydrous normalized data).

Element	<180 μm Fraction n = 46 [†]				180-2000 μm Fraction n = 47			
	Mean	Min	Max	SDp	Mean	Min	Max	SDp
<i>Major elements (wt%)</i>								
SiO ₂	63.64	54.14	71.57	3.52	72.49	58.88	81.96	4.52
TiO ₂	1.05	0.51	2.02	0.35	0.52	0.12	1.04	0.22
Al ₂ O ₃	16.25	12.78	21.55	1.99	13.85	10.13	25.84	2.63
Fe ₂ O ₃ t	9.68	3.55	21.92	3.70	5.14	1.05	14.76	3.12
MnO	0.21	0.11	0.44	0.06	0.11	0.05	0.26	0.05
MgO	1.52	0.66	2.29	0.37	0.88	0.40	1.66	0.29
CaO	2.55	1.09	3.79	0.60	1.69	0.63	3.11	0.51
Na ₂ O	2.63	0.40	4.59	0.98	2.30	0.93	3.69	0.68
K ₂ O	2.35	0.89	4.39	0.61	2.95	1.18	4.34	0.75
P ₂ O ₅	0.12	0.06	0.23	0.04	0.06	0.02	0.13	0.02
<i>Trace elements (ppm)</i>								
Ba	408.2	311.8	540.4	53.1	467.9	337.3	613.2	63.2
Ce	83.0	37.2	214.8	37.7	36.7	16.4	149.1	19.5
Cr	43.8	10.9	138.0	25.9	13.3	0.0	55.4	13.3
Ga	18.8	15.1	26.9	2.2	15.2	9.3	24.9	2.9
Nb	12.5	6.6	26.8	5.1	7.0	3.0	19.0	3.0
Ni	14.8	5.1	30.6	6.5	5.0	0.3	23.1	4.0
Pb	26.9	12.0	84.5	14.9	21.5	11.1	72.2	11.3
Rb	73.6	33.2	172.3	25.6	90.0	36.8	175.0	30.2
Sc	16.3	5.0	28.7	4.7	7.9	0.6	23.5	5.5
Sr	251.6	133.9	482.8	72.9	221.5	97.3	501.3	77.2
Th	16.8	4.9	61.2	13.3	6.8	2.4	29.9	4.2
V	228.1	50.6	573.1	121.2	103.2	6.5	355.2	83.9
Y	33.3	18.6	81.0	13.9	15.4	6.8	36.3	5.7
Zr	449.0	171.4	1250.0	271.7	123.2	65.3	331.1	45.8

Min Minimum
 Max Maximum
 SDp Population standard deviation

Notes: [†] one <180 μm sample could not be analyzed. Total iron as Fe₂O₃.

upper continental crust, although the <180 μm fraction shows slight enrichment in some ferromagnesian elements (Sc, Fe₂O₃t, TiO₂, V) and in Zr, Th, and Y. In both fractions, Nb, CaO, Na₂O, Sr, Rb, MgO and Ni are somewhat depleted relative to UCC.

Acknowledgements

Our thanks to Akihiro Takahashi, Edier Aristizabal and Balmer Echeverry for their assistance during fieldwork, and to Yoshihiro Sawada for access to the XRF.

References

- Avila, P.F., Santos, J.M., Ferreira, E. and Cardoso, E., 2005, Geochemical signatures and mechanisms of trace elements dispersion in the area of the Vale Das Gatas mine (Northern Portugal). *Journal of Geochemical Exploration*, **85**, 17-29.
- Basu, A.R., Sharma, M. and DeCelles, P.G., 1990, Nd, Sr-isotopic provenance and trace element geochemistry of Amazonian foreland basin fluvial sands, Bolivia and Peru: implications for ensialic Andean orogeny. *Earth and Planetary Science Letters*, **100**, 1-17.
- Condie, K. C., 1993, Chemical composition and evolution of the upper continental crust: Contrasting results from surface samples and shales.
- Chemical Geology, **104**, 1-37.
- Dinelli, E., Lucchini, F., Mordini, A. and Paganelli, L., 1999, Geochemistry of Oligocene-Miocene sandstones of the northern Apennines (Italy) and evolution of chemical features in relation to provenance changes. *Sedimentary Geology*, **127**, 193-207.
- Editorial Board of Geological Map of Shimane Prefecture (EBGMSP), 1997, Geological map of Shimane Prefecture (1:200,000).
- Iizumi, S., Mishima, H., Okamoto, Y. and Honma, H., 1984, A strontium isotope study on the Neu granitic pluton and its mafic inclusion, San'in zone, Southwest Japan. *Journal of the Japanese Association of Mineralogists, Petrologists and Economic Geologists*, **79**, 89-100.
- Johnsson, M.J., 1993, The system controlling the composition of clastic sediments. *Geological Society of America Special Paper*, **284**, 1-19.
- Kagami, H., Iizumi, S., Tainoshio, Y. and Owada, M., 1992, Spatial variation of Sr and Nd isotope ratios of Cretaceous-Paleogene granitoid rocks, Southwest Japan Arc. *Contributions to Mineralogy and Petrology*, **112**, 165-77.
- Kano, K., Yamauchi, S., Takayasu, K., Matsuura, H. and Bunno, M., 1994, Geology of the Matsue district, with Geological Sheet Map at scale 1:50,000. Tsukuba, Geological Survey of Japan, 126 p.*
- Kimura, J.I. and Yamada, Y., 1996, Evaluation of major and trace element analyses using a flux to sample ratio of two to one glass beads. *Journal of Mineralogy, Petrology and Economic Geology*, **91**, 62-72.
- Ohta, A., Imai, N., Terashima, S., Tachibana, Y., Ikebara, K. and Nakajima, T., 2004, Geochemical mapping in Hokuriku, Japan: influence of surface geology, mineral occurrences and mass movement from terrestrial to marine environments. *Applied Geochemistry*, **19**, 1453-1469.
- Ortiz, E. and Roser, B.P., 2003, Major and trace element abundances in the

- <180 μm fractions of stream sediments from the Kando River, Shimane Prefecture, Japan. *Geoscience Reports of Shimane University*, **22**, 111-120.
- Ortiz, E. and Roser, B.P., 2004a, Major and trace element abundances in the sand fractions of stream sediments from the Kando River, Shimane Prefecture, Japan. *Geoscience Reports of Shimane University*, **23**, 17-25.
- Ortiz, E. and Roser, B.P. 2004b, Major and trace element abundances in the <180 μm and sand fractions of stream sediments from the Hino River, Tottori, Japan. *Geoscience Reports of Shimane University*, **23**, 27-37.
- Roser, B.P., Kimura, J.-I. and Hisatomi, K., 2000, Whole-rock elemental abundances in sandstones and mudrocks from the Tanabe Group, Kii Peninsula, Japan. *Geoscience Reports of Shimane University*, **19**, 101-112.
- Roser, B.P., Tateishi, Y. and Nakayama, K., 2001, Whole-rock geochemical compositions of Miocene sedimentary and volcanic rocks from the Izumo-Matsue districts and Shimane Peninsula, SW Japan. *Geoscience Reports of Shimane University*, **20**, 69-82.
- Taylor, S.R. and McLennan, S.M., 1985, *The continental crust: its composition and evolution*. Blackwell, Oxford, 312 p.
- Tokuoka, T., Takayasu, K., Kunii, H., Takehiro, F. and Sampei, Y., 1998, Improving lagoonal environments for future generations -a case study of lakes Nakumi and Shinji, Japan-. *Laguna*, **5**, 1-10.
- Yamauchi, S. and Yoshitani A., 1992, Miocene tectonics of the southern Japan Sea and its adjacent area. *Memoirs of the Geological Society of Japan*, **37**, 311-326.*
- * In Japanese with English abstract or summary.

(要 旨)

Edwin Ortiz・Barry Roser, 島根県斐伊川から採取した河川堆積物の粒径 180 μm 以下と 180-2000 μm フラクションにおける主・微量元素組成. 地球資源環境学研究報告, **24**, 53-58

島根県の斐伊川の 47 ヶ所から採取した河川堆積物を篩いがけして粒径 180 μm 以下と 180-2000 μm フラクションに分離し, 主・微量元素組成の蛍光 X 線分析を行った。元素組成はこれら 2 つのフラクションによって明瞭な違いを示した。SiO₂, K₂O, Ba, Rb の平均含有量は粒径 180-2000 μm フラクションの方が 180 μm 以下より多いが, これ以外の元素では一般に低い。灼熱減量でも粒径 180 μm 以下の方がより大きい。両フラクションにおける平均組成は最上部大陸地殻の平均組成に類似している。最上部大陸地殻組成との大きな組成的違いは粒径 180 μm 以下のフラクションで認められ, それらはある種の苦鉄質元素(V, TiO₂, Fe₂O₃, Sc)と Zr, Y, Th に富んでいる。両フラクションにおいて, Nb, CaO, Na₂O, Sr, Rb, MgO, Ni は最上部大陸地殻(UCC)の平均組成に比べてわずかに少なくなっている。